



OPEN

Connexin43 and connexin50 channels exhibit different permeability to the second messenger inositol triphosphate

Virginijus Valiunas & Thomas W. White[✉]

Gap junction channels made of different connexins have distinct permeability to second messengers, which could affect many cell processes, including lens epithelial cell division. Here, we have compared the permeability of IP₃ and Ca²⁺ through channels made from two connexins, Cx43 and Cx50, that are highly expressed in vertebrate lens epithelial cells. Solute transfer was measured while simultaneously monitoring junctional conductance via dual whole-cell/perforated patch clamp. HeLa cells expressing Cx43 or Cx50 were loaded with Fluo-8, and IP₃ or Ca²⁺ were delivered via patch pipette to one cell of a pair, or to a monolayer while fluorescence intensity changes were recorded. Cx43 channels were permeable to IP₃ and Ca²⁺. Conversely, Cx50 channels were impermeable to IP₃, while exhibiting high permeation of Ca²⁺. Reduced Cx50 permeability to IP₃ could play a role in regulating cell division and homeostasis in the lens.

The proper growth and development of vertebrate tissues relies upon chemical communication between adjacent cells. This can result from the activation of cytoplasmic signal transduction cascades by extracellular growth factors to generate second messengers, or can directly occur between adjacent cells through the gap junction channels that link their cytoplasm. Both gap junctional communication and growth factor signaling pathways have been shown to play critical roles in the development and growth of the lens^{1–9}. However, few studies have examined if differential permeability to second messenger molecules by the connexin channels expressed in the lens epithelium, Cx43 and Cx50, could play a role in the specificity of cell-to-cell communication during eye development^{10–12}.

Initial reports assumed that gap junction channels would be relatively non-selective^{13,14}, however connexin-dependent differences in ion and small molecule permeability were subsequently identified^{15–18}. Further studies extended connexin permeation differences to second messenger molecules such as IP₃ and cAMP^{10,19–23}. Currently, it is thought that each type of connexin channel has functionally distinct ionic conductance and small molecule permeability^{19,20,24–26}. The importance of permeation differences between connexin channel types *in vivo* has been suggested by mouse genetic studies showing that loss of one connexin often cannot be compensated for by replacement with another^{27–32}.

Animal models with genetic manipulations of Cx43 and Cx50 have consistently supported this idea^{28,33–37}, and the lens is an excellent model system to explore differential permeability of gap junctions to second messengers. There is a well-established literature on the pathological effects resulting from genetically manipulating the lens connexins *in vivo*^{38–41}, that can be contrasted with changes in second messenger permeation observed *in vitro*. Here, we have used a combined patch clamp electrophysiological and fluorescent imaging approach to compare the permeation of IP₃ and Ca²⁺ through Cx43 and Cx50 channels *in vitro*. We found that Cx43 channels were permeable to both IP₃ and Ca²⁺, whereas channels composed of Cx50 showed undetectable permeability to IP₃, but high permeability to Ca²⁺ ions that was comparable to that of Cx43.

The Department of Physiology and Biophysics, Stony Brook University School of Medicine, Stony Brook, NY, 11794, USA. ✉e-mail: thomas.white@stonybrook.edu

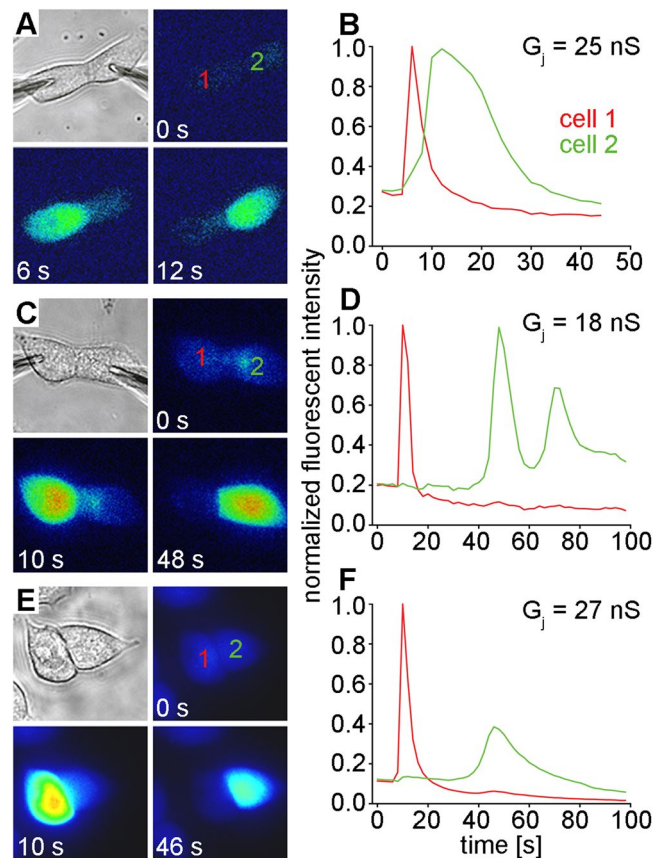


Figure 1. Cx43 channels are permeable to IP_3 . Three different Cx43 cell pairs are shown (A,C,E) that all showed increased Ca^{2+} fluorescence in cell 1 (red lines) when IP_3 was introduced, and 10 to 40 seconds later a response in cell 2 (green lines) after it had permeated through Cx43 channels (B,D,F). In the pairs shown in A-D, $500 \mu\text{M}$ IP_3 was in the pipette. In the pair shown in E-F, $250 \mu\text{M}$ IP_3 was in the pipette. The mean gap junctional conductance (\pm SD) for the three Cx43 cell pairs shown was 23 ± 4.7 nS.

Results

Cx43 channels are permeable to IP_3 . Permeability of connexin channels to IP_3 has been documented in a number of experimental systems, most frequently for channels composed of Cx26^{21–23,42–44}. Many of these studies utilized IP_3 mediated ER calcium release^{45,46} and Ca^{2+} sensitive fluorescent dyes to detect IP_3 permeation through gap junction channels. We analyzed the IP_3 permeability of Cx43 channels using cell pairs loaded with the Ca^{2+} binding dye Fluo-8 (Fig. 1). In all examples shown, cell 1 was patched in whole cell mode and IP_3 was added to the pipette solution. Cell 2 was patched in the perforated patch mode to simultaneously measure gap junctional conductance while imaging cell fluorescence (for experimental details see Materials and Methods). Cell fluorescence was initially monitored for 15–40 seconds to establish a baseline, then the whole cell mode with the pipette attached to cell 1 was established to release $500 \mu\text{M}$ IP_3 into the cytoplasm. A rapid spike in fluorescent intensity was observed in cell 1 (red traces), which rapidly attenuated due to the presence of 10 mM EGTA in the pipette solution. For every cell pair expressing Cx43 that we tested ($n = 16$), cell 2 showed a spike in fluorescent intensity (green traces) between 10 and 40 seconds after IP_3 was delivered to cell 1, indicating permeation through Cx43 gap junction channels. In rare cell pairs (Fig. 1C,D), the fluorescent response in the recipient cell showed Ca^{2+} oscillation, although we cannot conclusively explain why this occurred. In these cases, the first major response was counted as the positive result. In the third cell pair shown (Fig. 1E,F), the concentration of IP_3 in the pipette solution was reduced to $250 \mu\text{M}$. There were no statistically significant differences in the mean times (\pm SD) between the fluorescent peaks observed in cell 1 and cell 2 when the IP_3 concentration in the pipette solution was varied (16.2 ± 10.6 seconds, $n = 9$, for $500 \mu\text{M}$ versus 18.9 ± 11.3 seconds, $n = 7$ for $250 \mu\text{M}$, $p = 0.64$, student's t -test). The mean gap junctional conductance (\pm SD) for all of the Cx43 cell pairs investigated as shown in Fig. 1 was 21 ± 9.7 nS ($n = 16$).

IP_3 cannot permeate Cx50 channels. When we analyzed the IP_3 permeability of Cx50 channels using the same method (Fig. 2), a rapid spike in fluorescent intensity was observed in cell 1 (red traces), which rapidly attenuated, just as we had observed for Cx43. In contrast to Cx43, for every cell pair expressing Cx50 that we tested ($n = 18$), cell 2 never showed any spike in fluorescent intensity (green traces) for up to 220 seconds following IP_3 delivery to cell 1, indicating no detectable permeation of this second messenger through Cx50 gap junction channels. In the third cell pair shown (Fig. 2E,F), we directly introduced $500 \mu\text{M}$ IP_3 into cell 2 after

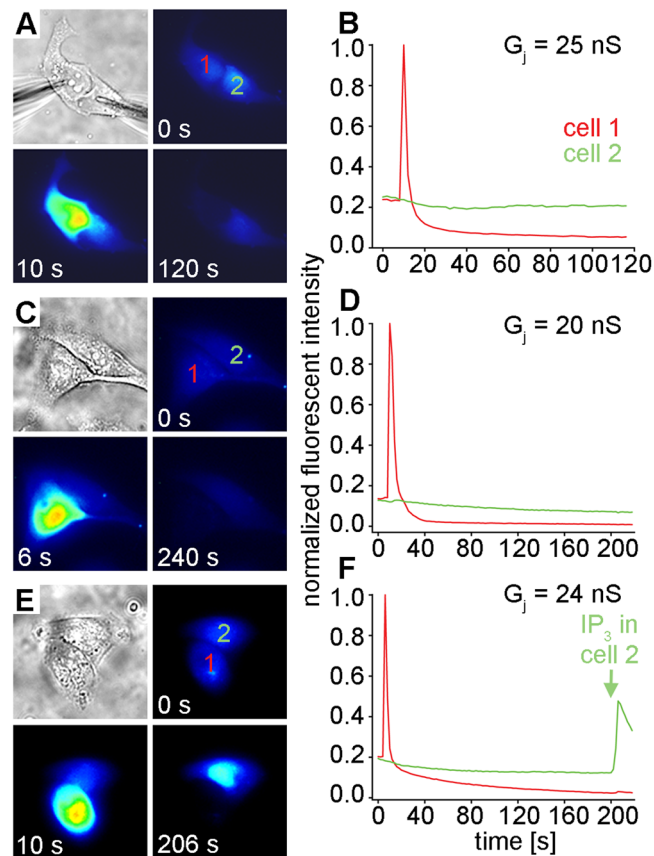


Figure 2. IP₃ does not permeate channels made of Cx50. Three different Cx50 cell pairs (A,C,E) all showed a rapid spike in Ca²⁺ fluorescent intensity in cell 1 (red lines) when IP₃ was introduced. In contrast to Cx43, cell 2 (green lines) never showed any spike in fluorescent intensity (B,D,E) for up to 220 seconds following IP₃ delivery to cell 1, indicating no permeation through Cx50 channels. When 500 μM IP₃ was directly introduced into cell 2 after monitoring fluorescence for 200 seconds following IP₃ release into cell 1 (E,F), a rapid spike in fluorescent intensity was observed in cell 2 within seconds. The mean gap junctional conductance (± SD) for the three Cx50 cell pairs shown was 23 ± 2.6 nS.

monitoring fluorescence for 200 seconds following IP₃ release into cell 1. We observed a rapid spike in fluorescent intensity in cell 2 within seconds, demonstrating that cell 2 was capable of responding to IP₃, and that the lack of response was due to the absence of its permeation through Cx50 channels. The mean gap junctional conductance (± SD) for all of the Cx50 cell pairs tested as shown in Fig. 2 was 21 ± 11.6 nS (n = 18), the same magnitude of coupling provided by Cx43 channels in the data presented in Fig. 1.

Cx43 and Cx50 channels are permeable to Ca²⁺. Connexin channels have been shown to be both permeable to and gated by Ca²⁺^{44,47–50}. For the lens connexins, physiologically relevant changes in the levels of cytoplasmic calcium have been reported to markedly reduce gap junctional coupling^{51,52}. To ensure that differential effects of Ca²⁺ on conductance of the two channel types did not cause the striking disparity in IP₃ permeability observed between Cx43 and Cx50, we examined the Ca²⁺ permeability and gating of Cx50 using cell pairs loaded with Fluo-8 (Fig. 3). Cell 1 was patched in whole cell mode and 2 mM Ca²⁺ was added to the pipette solution. Cell 2 was patched in whole cell mode to simultaneously measure gap junctional conductance while continuously imaging Fluo-8 fluorescence. Fluorescence was initially monitored for 10–30 seconds to establish a baseline, then the patch was ruptured under the pipette attached to cell 1 to establish the whole cell mode and to release Ca²⁺ into the cytoplasm. A rapid rise in fluorescent intensity was observed in cell 1 (red trace), which persisted due to the omission of 10 mM EGTA from the pipette solution. For every cell pair expressing Cx50 that we tested (n = 4), cell 2 showed a rise in fluorescent intensity (green traces) between ~ 5 and 20 seconds after Ca²⁺ was delivered to cell 1, indicating permeation through Cx50 gap junction channels. The simultaneous measurement of gap junctional conductance showed that Cx50 was also gated by Ca²⁺, as was previously documented⁵³, although on a much slower timescale than the solute permeation. A ~50% decline in the Cx50 junctional current was observed 60 seconds after 2 mM Ca²⁺ was delivered to cell 1, which increased to a 77% decline in coupling at 180 seconds. The mean gap junctional conductance (± SD) for all of the Cx50 cell pairs used in calcium permeability studies was 14 ± 5.1 nS.

We also found that Cx43 channels were highly permeable to Ca²⁺, although we used a more simplified assay (Fig. 4A,B, n = 5). In these experiments, Cx43 expressing cells were loaded with Fluo-8 and a single cell in a multicellular cluster was patched in the whole cell mode with 2 mM Ca²⁺ added to the pipette solution while

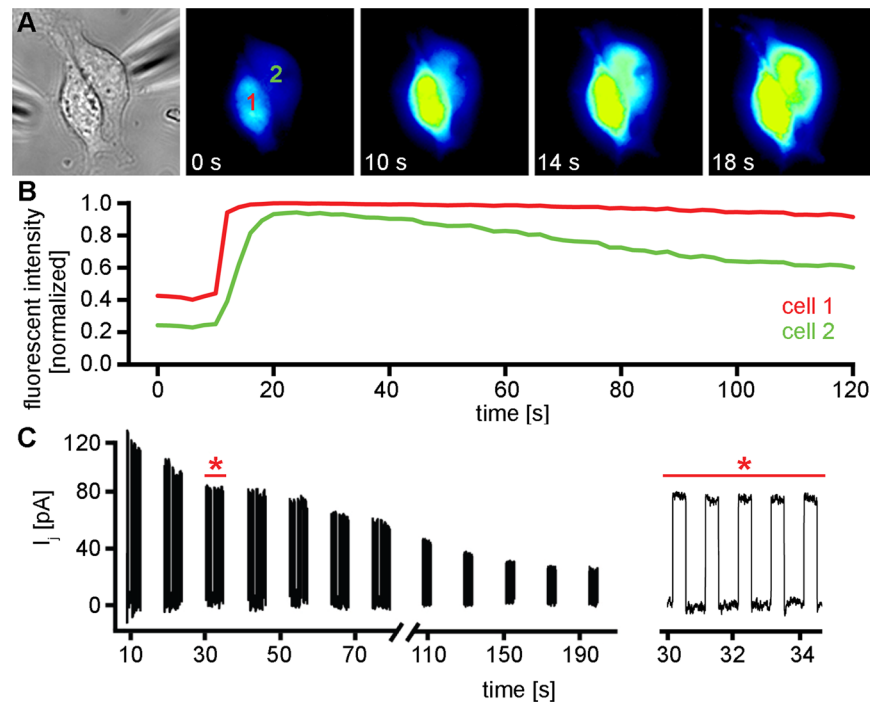


Figure 3. Cx50 Channels are permeable to Ca^{2+} ions. A cell pair expressing Cx50 (A), showed a strong fluorescent response in cell 1 (B, red line), when the pipette attached to cell 1 was opened to release 2 mM Ca^{2+} into the cytoplasm. Cell 2 showed a rise in fluorescent intensity (B, green line) that reached a peak within 10 seconds after Ca^{2+} was delivered to cell 1. Simultaneous measurement of gap junctional currents (C) showed that Cx50 was gated by Ca^{2+} on a much slower time scale than the solute permeation. A less than 50% decline in the Cx50 junctional current was seen 60 seconds after 2 mM Ca^{2+} was delivered to cell 1, which increased to a 77% decline in coupling at 180 seconds. An expanded portion of the record (red asterisk) showed that junctional currents remained stable for many seconds after peak Ca^{2+} transfer had occurred.

fluorescence was continuously monitored. Fluo-8 fluorescence rapidly increased in the patched cell, followed by a fluorescence increase in more distal cells in contact with the patched cell within one minute. Similar results were obtained with Cx50 expressing cells, when 2 mM Ca^{2+} was introduced into the cytoplasm of a single cell within a large cluster of cells (Fig. 4C,D, $n = 3$). For these Ca^{2+} permeability studies, 10 mM EGTA was omitted from the pipette solution. In contrast, delivery of 500 μM IP_3 into the cytoplasm of a single cell within a large cluster of Cx50 expressing cells resulted in a rapid peak of fluorescent intensity in the injected cell, with no evidence of IP_3 permeation to adjacent cells (Fig. 4E, $n = 3$). For these IP_3 permeability studies, 10 mM EGTA was present in the pipette solution. These results confirmed that while both Cx43 and Cx50 channels showed a high permeability to Ca^{2+} , only Cx43 displayed detectable permeability to the second messenger IP_3 .

Discussion

We have contrasted IP_3 and Ca^{2+} permeability through gap junction channels formed from the lens connexins, Cx43 and Cx50. Cx50 showed greatly reduced IP_3 permeability compared to Cx43, while both connexins were readily permeable to Ca^{2+} . Differences in the permeation of these second messengers through Cx43 and Cx50 channels could influence the development of cataract in the lens. Calcium has long been known to play a significant role in cataract formation^{54,55} and altered Ca^{2+} signaling in lens epithelial cells has been implicated in cataract progression⁵⁶. In addition, the lens possesses an array of G-protein coupled receptors that facilitate the release of intracellular calcium through the generation of IP_3 ⁵⁷⁻⁵⁹ and gap junction mediated Ca^{2+} signaling has been documented in primary cultures of lens epithelial cells⁶⁰. Since the intercellular movement of IP_3 appears to be more important for cell-to-cell propagation of Ca^{2+} signals^{43,61} (supplementary Fig. S1), the profoundly different permeability of Cx43 and Cx50 to IP_3 could be relevant in cataract progression in the lens.

Differential permeability of IP_3 through Cx43 and Cx50 channels could also impact lens cell proliferation and growth during development. Cx50 knockout decreased epithelial cell division during the first post-natal week, resulting in a significant reduction of lens growth^{7,34,62}. In contrast, deletion of Cx43 did not reduce lens growth^{36,63}, suggesting that a specific functional difference between Cx43 and Cx50 was required for normal post-natal epithelial mitosis and lens growth to occur. IP_3 and Ca^{2+} act synergistically to influence cell division⁶⁴⁻⁶⁶, including in cultured human lens epithelial cells⁶⁷. Elevated IP_3 levels lead to Ca^{2+} release from the endoplasmic reticulum⁶⁸, potentially linking second messenger generation following receptor activation to permeability properties of connexin channels. If restricted IP_3 permeability through connexin channels were important for normal epithelial cell division during postnatal development, then one would predict that Cx43 could not compensate for loss of Cx50 in the lens epithelium, as it exhibits much greater permeability to IP_3 .

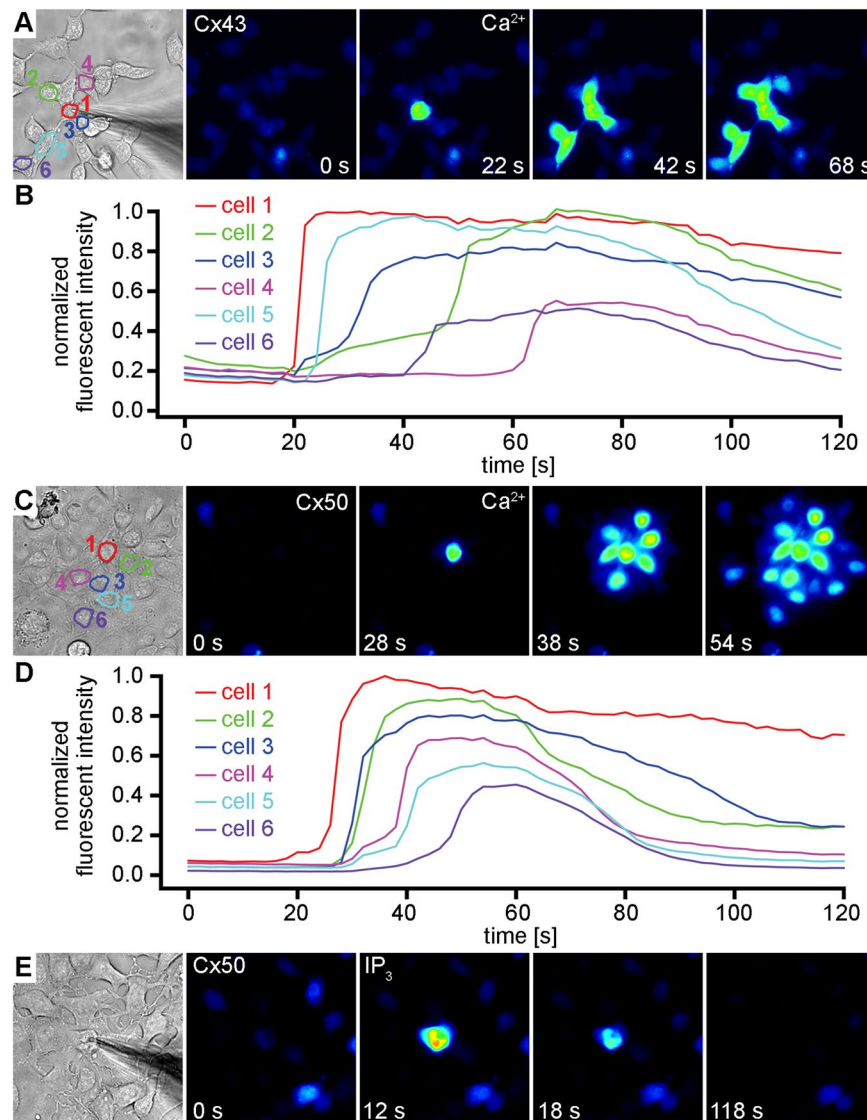


Figure 4. Ca²⁺ and IP₃ permeation in monolayer cultures of Cx43 and Cx50 expressing cells. After recording background fluorescence for ~20 seconds, 2 mM Ca²⁺ was released into a single cell in a cluster of Cx43 expressing cells loaded with Fluo-8 (A). Fluorescence rapidly increased in the patched cell, followed by an increase in 5 more distal cells (B) within 60 seconds. Similar (C–D) results were obtained when 2 mM Ca²⁺ was introduced into the cytoplasm of a single cell within a cluster of Cx50 expressing cells. In contrast, delivery of 500 μM IP₃ into the cytoplasm of a single cell within a cluster of Cx50 expressing cells (E) resulted in a rapid peak of fluorescent intensity in the injected cell, with no evidence of IP₃ permeation to any of the adjacent cells.

Recently, the structure of Cx50 has been resolved by cryo-electron microscopy at a resolution near the atomic level (~3.4 Å)⁶⁹. Although there is no equivalent structure of Cx43 at this resolution, the availability of a Cx50 structure may allow approaches such as comparative all-atom MD simulations to probe isoform-specific differences in perm-selectivity to second messengers like IP₃. Cx26 has been shown to be permeable to IP₃^{22,43}, and there is also an atomic level structure for this connexin⁷⁰, so this approach would not absolutely require an atomic level structure of Cx43. The documentation of profound differences in the permeation of connexin channels to biologically relevant second messengers is an important step in understanding the need for connexin diversity to maintain homeostasis in a variety of biological systems^{29,71}. In combination with increasing information about connexin channel atomic structure, the molecular basis for these permeability differences may finally be elucidated in future studies.

Materials and Methods

Cell lines. HeLa cells that had been previously stably transfected with rat Cx43, or human Cx50^{17,72} were cultured and plated as described¹⁰. Briefly, cells were grown in DMEM (Gibco/Thermo Fisher Scientific, Waltham, MA), supplemented with 10% FCS (Hyclone/ Thermo Fisher Scientific, Waltham, MA), 100 μg/mL streptomycin, and 100 U/mL penicillin (Gibco) and were passaged weekly, diluted 1:10, and kept at 37 °C in a CO₂ incubator

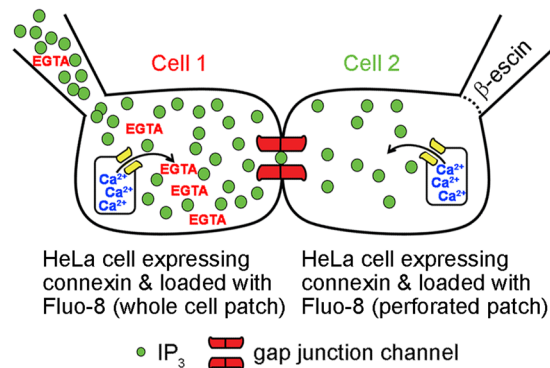


Figure 5. An assay for intercellular transfer of IP₃ through gap junction channels. Cell pairs are cultured where both cells express the connexin to be tested, and are loaded with the Ca²⁺ indicator Fluo-8. 500 μM IP₃ is delivered via patch pipette into cell 1 in whole cell mode, and Fluo-8 fluorescence is continuously recorded in both cells using a digital camera. When IP₃ transfers to cell 2 through connexin channels, the liberation of Ca²⁺ from ER stores can be detected. Cell 2 is patched in the perforated mode to simultaneously record junctional conductance.

(5% CO₂ / 95% ambient air). Permeability measurements were carried out on cell pairs plated on glass coverslips at low density.

Patch clamp electrophysiology. A combined whole-cell/perforated patch dual voltage-clamp method was used to measure gap junctional conductance between cell pairs^{17,73}. Coverslips with cells expressing Cx43, or Cx50, were transferred to a recording chamber on an inverted microscope with a fluorescence imaging system. Cells were perfused with a solution containing (in mM) NaCl, 150; KCl, 10; CaCl₂, 2; HEPES, 5 (pH 7.4); glucose, 5; CsCl, 2; and BaCl₂, 2. Patch clamp electrodes were filled with a solution containing (in mM) K⁺ aspartate⁻, 120; NaCl, 10; MgATP, 3; HEPES, 5 (pH 7.2); EGTA, 10. For electrodes used in a perforated patch configuration, the solution was supplemented with 30–50 μM β-escin⁷⁴. Patch clamp electrodes were pulled from glass capillaries (Harvard Apparatus, Holliston, MA) with a horizontal puller (DMZ-Universal, Zeitz-Instrument, Martinsried, Germany). The measured resistance of the electrodes was 2–5 MΩ. Gap junctional conductance was measured throughout each experiment, beginning when both cells in the pair had been successfully patched.

IP₃ permeability studies. We used IP₃ mediated ER calcium release^{45,46} and Ca²⁺ sensitive fluorescent dyes as an assay for IP₃ permeation through gap junction channels (Fig. 5). The detection of intercellular IP₃ transfer was accomplished by culturing cell pairs where both cells expressed the connexin to be tested, and were pre-loaded with the calcium indicator dye Fluo-8 (5 μM, AAT Bioquest, Sunnyvale, CA) according to the manufacturer's protocol. IP₃ transfer was monitored by continuously recording fluorescence in both cells using a digital CCD-camera (HRm Axiocam, Carl Zeiss, Thornwood, NY), while simultaneously measuring junctional conductance between cells 1 & 2 after the delivery of 250 or 500 μM IP₃ to cell 1 through the patch pipette. An outline of each cell, and an equally sized area of background in an adjacent area without cells, were manually drawn in the images using AxioVision Software (Carl Zeiss, White Plains, NY). Fluorescent intensities for recipient and source cells were corrected by subtracting the background intensity, normalized to the peak fluorescent intensity in cell 1 and plotted versus time. To ensure that we monitored the passage of IP₃, and not endogenous free Ca²⁺, which would also be liberated in the source cell, the pipette solution contained 10 mM EGTA to chelate the released Ca²⁺ in cell 1, and prevent its passage to cell 2 through gap junction channels. However, previous reports^{43,61,75,76} and additional control experiments (Supplementary Figure S1) suggested that the cell-to-cell transfer of endogenous Ca²⁺ was likely too minimal to confound our ability to detect IP₃ transfer. Cell 2 was recorded in the perforated patch mode to prevent IP₃ from diffusing into the recipient cell pipette. To prevent endogenous IP₃ synthesis or degradation within the source cell, 3.5 mM diphosphoglyceric acid (a competitive inhibitor of IP₃ phosphomonoesterases) and 20 μM IP₃-kinase inhibitor (MilliporeSigma, Burlington, MA) were included in the pipette solution^{42,77}.

Ca²⁺ permeability studies. Connexin expressing cell pairs loaded with Fluo-8 were also used to directly monitor Ca²⁺ permeability through gap junction channels. The detection of intercellular Ca²⁺ transfer was accomplished by culturing cell pairs where both cells expressed the connexin to be tested, and were pre-loaded with Fluo-8. Ca²⁺ transfer was monitored by continuously recording fluorescence in both cells, while simultaneously measuring junctional conductance between cells 1 & 2 after the delivery of 2 mM Ca²⁺ to cell 1. In some experiments, a single cell in a multicellular cluster of connexin cells was patched in the whole cell mode with 2 mM Ca²⁺ added to the pipette solution while Fluo-8 fluorescence was continuously monitored in the entire field of adjacent cells. For these studies, 10 mM EGTA was omitted from the pipette solution.

Received: 28 January 2020; Accepted: 7 May 2020;

Published online: 26 May 2020

References

- Gerido, D. A. & White, T. W. Connexin disorders of the ear, skin, and lens. *Biochim Biophys Acta* **1662**, 159–170, <https://doi.org/10.1016/j.bbamem.2003.10.017> (2004).
- Lovicu, F. J. Cell signaling in lens development. *Semin Cell Dev Biol* **17**, 675, <https://doi.org/10.1016/j.semcdb.2006.10.003> (2006).
- McAvoy, J. W., Chamberlain, C. G., de Jongh, R. U., Hales, A. M. & Lovicu, F. J. Lens development. *Eye (Lond)* **13**(Pt 3b), 425–437, <https://doi.org/10.1038/eye.1999.117> (1999).
- Robinson, M. L. An essential role for FGF receptor signaling in lens development. *Semin Cell Dev Biol* **17**, 726–740, <https://doi.org/10.1016/j.semcdb.2006.10.002> (2006).
- Boswell, B. A., Lein, P. J. & Musil, L. S. Cross-talk between fibroblast growth factor and bone morphogenetic proteins regulates gap junction-mediated intercellular communication in lens cells. *Mol Biol Cell* **19**, 2631–2641, <https://doi.org/10.1091/mbc.E08-02-0124> (2008).
- Le, A. C. & Musil, L. S. A novel role for FGF and extracellular signal-regulated kinase in gap junction-mediated intercellular communication in the lens. *J Cell Biol* **154**, 197–216 (2001).
- Sellitto, C., Li, L. & White, T. W. Connexin50 is essential for normal postnatal lens cell proliferation. *Invest Ophthalmol Vis Sci* **45**, 3196–3202, <https://doi.org/10.1167/iovs.04-0194> (2004).
- Sellitto, C. *et al.* The Phosphoinositide 3-Kinase Catalytic Subunit p110alpha is Required for Normal Lens Growth. *Invest Ophthalmol Vis Sci* **57**, 3145–3151, <https://doi.org/10.1167/iovs.16-19607> (2016).
- Berthoud, V. M. & Ngezahayo, A. Focus on lens connexins. *BMC Cell Biol* **18**, 6, <https://doi.org/10.1186/s12860-016-0116-6> (2017).
- Valiunas, V., Brink, P. R. & White, T. W. Lens Connexin Channels Have Differential Permeability to the Second Messenger cAMP. *Invest Ophthalmol Vis Sci* **60**, 3821–3829, <https://doi.org/10.1167/iovs.19-27302> (2019).
- White, T. W., Gao, Y., Li, L., Sellitto, C. & Srinivas, M. Optimal lens epithelial cell proliferation is dependent on the connexin isoform providing gap junctional coupling. *Invest Ophthalmol Vis Sci* **48**, 5630–5637, <https://doi.org/10.1167/iovs.06-1540> (2007).
- Dahm, R., van Marle, J., Prescott, A. R. & Quinlan, R. A. Gap junctions containing alpha8-connexin (MP70) in the adult mammalian lens epithelium suggests a re-evaluation of its role in the lens. *Exp Eye Res* **69**, 45–56, <https://doi.org/10.1006/exer.1999.0670> (1999).
- Goodenough, D. A. Gap junction dynamics and intercellular communication. *Pharmacol Rev* **30**, 383–392 (1978).
- Gilula, N. B., Reeves, O. R. & Steinbach, A. Metabolic coupling, ionic coupling and cell contacts. *Nature* **235**, 262–265 (1972).
- Goldberg, G. S., Valiunas, V. & Brink, P. R. Selective permeability of gap junction channels. *Biochim Biophys Acta* **1662**, 96–101, <https://doi.org/10.1016/j.bbamem.2003.11.022> (2004).
- Kanaporis, G., Brink, P. R. & Valiunas, V. Gap junction permeability: selectivity for anionic and cationic probes. *Am J Physiol Cell Physiol* **300**, C600–609, <https://doi.org/10.1152/ajpcell.00316.2010> (2011).
- Valiunas, V., Beyer, E. C. & Brink, P. R. Cardiac gap junction channels show quantitative differences in selectivity. *Circ Res* **91**, 104–111 (2002).
- Veenstra, R. D. *et al.* Selectivity of connexin-specific gap junctions does not correlate with channel conductance. *Circ Res* **77**, 1156–1165 (1995).
- Kanaporis, G. *et al.* Gap junction channels exhibit connexin-specific permeability to cyclic nucleotides. *J Gen Physiol* **131**, 293–305, <https://doi.org/10.1085/jgp.200709934> (2008).
- Mese, G., Valiunas, V., Brink, P. R. & White, T. W. Connexin26 deafness associated mutations show altered permeability to large cationic molecules. *Am J Physiol Cell Physiol* **295**, C966–974, <https://doi.org/10.1152/ajpcell.00008.2008> (2008).
- Ayad, W. A., Locke, D., Koreen, I. V. & Harris, A. L. Heteromeric, but not homomeric, connexin channels are selectively permeable to inositol phosphates. *J Biol Chem* **281**, 16727–16739, <https://doi.org/10.1074/jbc.M600136200> (2006).
- Beltramello, M., Piazza, V., Bukauskas, F. F., Pozzan, T. & Mammano, F. Impaired permeability to Ins(1,4,5)P₃ in a mutant connexin underlies recessive hereditary deafness. *Nat Cell Biol* **7**, 63–69, <https://doi.org/10.1038/ncb1205> (2005).
- Zhang, Y. *et al.* Gap junction-mediated intercellular biochemical coupling in cochlear supporting cells is required for normal cochlear functions. *Proc Natl Acad Sci USA* **102**, 15201–15206, <https://doi.org/10.1073/pnas.0501859102> (2005).
- Bukauskas, F. F. & Verselis, V. K. Gap junction channel gating. *Biochim Biophys Acta* **1662**, 42–60, <https://doi.org/10.1016/j.bbamem.2004.01.008> (2004).
- Harris, A. L. Connexin channel permeability to cytoplasmic molecules. *Prog Biophys Mol Biol* **94**, 120–143, <https://doi.org/10.1016/j.pbiomolbio.2007.03.011> (2007).
- Harris, A. L. Emerging issues of connexin channels: biophysics fills the gap. *Q Rev Biophys* **34**, 325–472 (2001).
- Plum, A. *et al.* Unique and shared functions of different connexins in mice. *Curr Biol* **10**, 1083–1091 (2000).
- White, T. W. Unique and redundant connexin contributions to lens development. *Science* **295**, 319–320, <https://doi.org/10.1126/science.1067582> (2002).
- White, T. W. Nonredundant gap junction functions. *News Physiol Sci* **18**, 95–99 (2003).
- Dicke, N. *et al.* Peripheral lymphangiogenesis in mice depends on ectodermal connexin-26 (Gjb2). *J Cell Sci* **124**, 2806–2815, <https://doi.org/10.1242/jcs.084186> (2011).
- Zheng-Fischhofer, Q. *et al.* Connexin31 cannot functionally replace connexin43 during cardiac morphogenesis in mice. *J Cell Sci* **119**, 693–701, <https://doi.org/10.1242/jcs.02800> (2006).
- Alcolea, S. *et al.* Replacement of connexin40 by connexin45 in the mouse: impact on cardiac electrical conduction. *Circ Res* **94**, 100–109, <https://doi.org/10.1161/01.RES.0000108261.67979.2A> (2004).
- Wang, E., Geng, A., Seo, R., Maniar, A. & Gong, X. Knock-in of Cx46 partially rescues fiber defects in lenses lacking Cx50. *Mol Vis* **23**, 160–170 (2017).
- White, T. W., Goodenough, D. A. & Paul, D. L. Targeted ablation of connexin50 in mice results in microphthalmia and zonular pulverulent cataracts. *J Cell Biol* **143**, 815–825 (1998).
- Rong, P. *et al.* Disruption of Gja8 (alpha8 connexin) in mice leads to microphthalmia associated with retardation of lens growth and lens fiber maturation. *Development* **129**, 167–174 (2002).
- White, T. W., Sellitto, C., Paul, D. L. & Goodenough, D. A. Prenatal lens development in connexin43 and connexin50 double knockout mice. *Invest Ophthalmol Vis Sci* **42**, 2916–2923 (2001).
- Martinez-Wittinghan, F. J. *et al.* Dominant cataracts result from incongruous mixing of wild-type lens connexins. *J Cell Biol* **161**, 969–978, <https://doi.org/10.1083/jcb.200303068> (2003).
- Yuan, L. *et al.* CRISPR/Cas9-mediated GJA8 knockout in rabbits recapitulates human congenital cataracts. *Sci Rep* **6**, 22024, <https://doi.org/10.1038/srep22024> (2016).
- Jiang, J. X. Gap junctions or hemichannel-dependent and independent roles of connexins in cataractogenesis and lens development. *Curr Mol Med* **10**, 851–863 (2010).
- Berthoud, V. M., Minogue, P. J., Osmolok, P., Snabb, J. I. & Beyer, E. C. Roles and regulation of lens epithelial cell connexins. *FEBS Lett* **588**, 1297–1303, <https://doi.org/10.1016/j.febslet.2013.12.024> (2014).
- Mathias, R. T., White, T. W. & Gong, X. Lens gap junctions in growth, differentiation, and homeostasis. *Physiol Rev* **90**, 179–206, <https://doi.org/10.1152/physrev.00034.2009> (2010).
- Hernandez, V. H. *et al.* Unitary permeability of gap junction channels to second messengers measured by FRET microscopy. *Nat Methods* **4**, 353–358, <https://doi.org/10.1038/nmeth1031> (2007).
- Niessen, H., Harz, H., Bedner, P., Kramer, K. & Willecke, K. Selective permeability of different connexin channels to the second messenger inositol 1,4,5-trisphosphate. *J Cell Sci* **113**(Pt 8), 1365–1372 (2000).

44. Saez, J. C., Connor, J. A., Spray, D. C. & Bennett, M. V. Hepatocyte gap junctions are permeable to the second messenger, inositol 1,4,5-trisphosphate, and to calcium ions. *Proc Natl Acad Sci USA* **86**, 2708–2712, <https://doi.org/10.1073/pnas.86.8.2708> (1989).
45. Gill, D. L., Ghosh, T. K. & Mullaney, J. M. Calcium signalling mechanisms in endoplasmic reticulum activated by inositol 1,4,5-trisphosphate and GTP. *Cell Calcium* **10**, 363–374 (1989).
46. Berridge, M. J. Inositol trisphosphate and calcium signalling mechanisms. *Biochim Biophys Acta* **1793**, 933–940, <https://doi.org/10.1016/j.bbamcr.2008.10.005> (2009).
47. De Mello, W. C. Effect of intracellular injection of calcium and strontium on cell communication in heart. *J Physiol* **250**, 231–245, <https://doi.org/10.1113/jphysiol.1975.sp011051> (1975).
48. Spray, D. C., Stern, J. H., Harris, A. L. & Bennett, M. V. Gap junctional conductance: comparison of sensitivities to H and Ca ions. *Proc Natl Acad Sci USA* **79**, 441–445, <https://doi.org/10.1073/pnas.79.2.441> (1982).
49. Rose, B. & Loewenstein, W. R. Permeability of cell junction depends on local cytoplasmic calcium activity. *Nature* **254**, 250–252, <https://doi.org/10.1038/254250a0> (1975).
50. Peracchia, C. Calmodulin-Mediated Regulation of Gap Junction Channels. *Int J Mol Sci* **21**, <https://doi.org/10.3390/ijms21020485> (2020).
51. Crow, J. M., Atkinson, M. M. & Johnson, R. G. Micromolar levels of intracellular calcium reduce gap junctional permeability in lens cultures. *Invest Ophthalmol Vis Sci* **35**, 3332–3341 (1994).
52. Lurtz, M. M. & Louis, C. F. Intracellular calcium regulation of connexin43. *Am J Physiol Cell Physiol* **293**, C1806–1813, <https://doi.org/10.1152/ajpcell.00630.2006> (2007).
53. Chen, Y. *et al.* Molecular interaction and functional regulation of connexin50 gap junctions by calmodulin. *Biochem J* **435**, 711–722, <https://doi.org/10.1042/BJ20101726> (2011).
54. Duncan, G. & Jacob, T. J. Calcium and the physiology of cataract. *Ciba Found Symp* **106**, 132–152 (1984).
55. Truscott, R. J., Marcantonio, J. M., Tomlinson, J. & Duncan, G. Calcium-induced opacification and proteolysis in the intact rat lens. *Invest Ophthalmol Vis Sci* **31**, 2405–2411 (1990).
56. Gosak, M. *et al.* The Analysis of Intracellular and Intercellular Calcium Signaling in Human Anterior Lens Capsule Epithelial Cells with Regard to Different Types and Stages of the Cataract. *PLoS One* **10**, e0143781, <https://doi.org/10.1371/journal.pone.0143781> (2015).
57. Duncan, G. & Wormstone, I. M. Calcium cell signalling and cataract: role of the endoplasmic reticulum. *Eye (Lond)* **13**(Pt 3b), 480–483, <https://doi.org/10.1038/eye.1999.125> (1999).
58. Rhodes, J. D. & Sanderson, J. The mechanisms of calcium homeostasis and signalling in the lens. *Exp Eye Res* **88**, 226–234, <https://doi.org/10.1016/j.exer.2008.10.025> (2009).
59. Vivekanandan, S. & Lou, M. F. Evidence for the presence of phosphoinositide cycle and its involvement in cellular signal transduction in the rabbit lens. *Curr Eye Res* **8**, 101–111 (1989).
60. Churchill, G. C., Atkinson, M. M. & Louis, C. F. Mechanical stimulation initiates cell-to-cell calcium signaling in ovine lens epithelial cells. *J Cell Sci* **109**(Pt 2), 355–365 (1996).
61. Sanderson, M. J., Charles, A. C., Boitano, S. & Dirksen, E. R. Mechanisms and function of intercellular calcium signaling. *Mol Cell Endocrinol* **98**, 173–187, [https://doi.org/10.1016/0303-7207\(94\)90136-8](https://doi.org/10.1016/0303-7207(94)90136-8) (1994).
62. Sikic, H., Shi, Y., Lubura, S. & Bassnett, S. A stochastic model of eye lens growth. *J Theor Biol* **376**, 15–31, <https://doi.org/10.1016/j.jtbi.2015.03.021> (2015).
63. DeRosa, A. M. *et al.* The cataract causing Cx50-S50P mutant inhibits Cx43 and intercellular communication in the lens epithelium. *Exp Cell Res* **315**, 1063–1075, <https://doi.org/10.1016/j.yexcr.2009.01.017> (2009).
64. Means, A. R. Calcium, calmodulin and cell cycle regulation. *FEBS Lett* **347**, 1–4, [https://doi.org/10.1016/0014-5793\(94\)00492-7](https://doi.org/10.1016/0014-5793(94)00492-7) (1994).
65. Lu, K. P. & Means, A. R. Regulation of the cell cycle by calcium and calmodulin. *Endocr Rev* **14**, 40–58, <https://doi.org/10.1210/edrv-14-1-40> (1993).
66. Whitaker, M. & Patel, R. Calcium and cell cycle control. *Development* **108**, 525–542 (1990).
67. Wang, L., Wormstone, I. M., Reddan, J. R. & Duncan, G. Growth factor receptor signalling in human lens cells: role of the calcium store. *Exp Eye Res* **80**, 885–895, <https://doi.org/10.1016/j.exer.2005.01.002> (2005).
68. Berridge, M. J., Lipp, P. & Bootman, M. D. The versatility and universality of calcium signalling. *Nat Rev Mol Cell Biol* **1**, 11–21, <https://doi.org/10.1038/35036035> (2000).
69. Myers, J. B. *et al.* Structure of native lens connexin 46/50 intercellular channels by cryo-EM. *Nature* **564**, 372–377, <https://doi.org/10.1038/s41586-018-0786-7> (2018).
70. Maeda, S. *et al.* Structure of the connexin 26 gap junction channel at 3.5 Å resolution. *Nature* **458**, 597–602, <https://doi.org/10.1038/nature07869> (2009).
71. Bruzzone, R., White, T. W. & Paul, D. L. Connections with connexins: the molecular basis of direct intercellular signaling. *Eur J Biochem* **238**, 1–27 (1996).
72. Berthoud, V. M. *et al.* Loss of function and impaired degradation of a cataract-associated mutant connexin50. *Eur J Cell Biol* **82**, 209–221, <https://doi.org/10.1078/0171-9335-00316> (2003).
73. Valiunas, V., Gemel, J., Brink, P. R. & Beyer, E. C. Gap junction channels formed by coexpressed connexin40 and connexin43. *Am J Physiol Heart Circ Physiol* **281**, H1675–1689 (2001).
74. Fan, J. S. & Palade, P. Perforated patch recording with beta-escin. *Pflugers Arch* **436**, 1021–1023 (1998).
75. Niessen, H. & Willecke, K. Strongly decreased gap junctional permeability to inositol 1,4, 5-trisphosphate in connexin32 deficient hepatocytes. *FEBS Lett* **466**, 112–114 (2000).
76. Yule, D. I., Stuenkel, E. & Williams, J. A. Intercellular calcium waves in rat pancreatic acini: mechanism of transmission. *Am J Physiol* **271**, C1285–1294, <https://doi.org/10.1152/ajpcell.1996.271.4.C1285> (1996).
77. Downes, C. P., Mussat, M. C. & Michell, R. H. The inositol trisphosphate phosphomonoesterase of the human erythrocyte membrane. *Biochem J* **203**, 169–177 (1982).

Acknowledgements

Supported by NIH Grants EY013163 & EY026911 to T.W.W., and GM088181 to V.V.

Author contributions

V.V. performed experiments, V.V. and T.W.W. designed experiments and contributed to data analysis, and T.W.W. wrote the manuscript. All authors reviewed the manuscript prior to submission.

Competing interests

The authors declare no competing interests.

Additional information

Supplementary information is available for this paper at <https://doi.org/10.1038/s41598-020-65761-z>.

Correspondence and requests for materials should be addressed to T.W.W.

Reprints and permissions information is available at www.nature.com/reprints.

Publisher's note Springer Nature remains neutral with regard to jurisdictional claims in published maps and institutional affiliations.



Open Access This article is licensed under a Creative Commons Attribution 4.0 International License, which permits use, sharing, adaptation, distribution and reproduction in any medium or format, as long as you give appropriate credit to the original author(s) and the source, provide a link to the Creative Commons license, and indicate if changes were made. The images or other third party material in this article are included in the article's Creative Commons license, unless indicated otherwise in a credit line to the material. If material is not included in the article's Creative Commons license and your intended use is not permitted by statutory regulation or exceeds the permitted use, you will need to obtain permission directly from the copyright holder. To view a copy of this license, visit <http://creativecommons.org/licenses/by/4.0/>.

© The Author(s) 2020